BIOCHEMISTRY
including biophysical chemistry & molecular biology

Article

pubs.acs.org/biochemistry

Role of Bilayer Characteristics on the Structural Fate of Aβ(1−40) and Aβ(25−40)

Jian Xiong, Carol A. Roach, Olayinka O. Oshokoya, Robert P. Schroell, Rauta A. Yakubu, Michael K. Eagleburger, Jason W. Cooley, and Renee D. JiJi*

Department of Chemistry, University of Missouri, Columbia, Missouri 65211, United States

ABSTRACT: The β-amyloid (Aβ) peptide is derived from the transmembrane (TM) helix of the amyloid precursor protein (APP) and has been shown to interact with membrane surfaces. To understand better the role of peptide−membrane interactions in cell death and ultimately in Alzheimer's disease, a better understanding of how membrane characteristics affect the binding, solvation, and secondary structure of Aβ is needed. Employing a combination of circular dichroism and deep-UV resonance Raman spectroscopies, Aβ(25−40) was found to fold spontaneously upon association with anionic lipid bilayers. The hydrophobic portion of the disease-related Aβ(1−40) peptide, Aβ(25−40), has often been used as a model for how its legacy TM region may behave structurally in aqueous solvents and during membrane encounters. The structure of the membrane-associated Aβ(25−40) peptide was found to depend on both the hydrophobic thickness of the bilayer and the duration of incubation. Similarly, the disease-related Aβ(1−40) peptide also spontaneously associates with anionic liposomes, where it initially adopts mixtures of disordered and helical structures. The partially disordered helical structures then convert to β-sheet structures over longer time frames. β-Sheet structure is formed prior to helical unwinding, implying a model in which β-sheet structure, formed initially from disordered regions, prompts the unwinding and destabilization of membrane-stabilized helical structure. A model is proposed to describe the mechanism of escape of Aβ(1−40) from the membrane surfaces following its formation by cleavage of APP within the membrane.

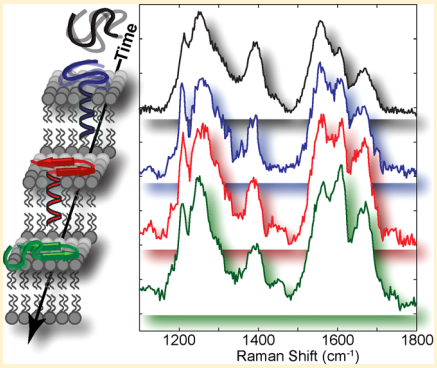

Alzheimer's disease (AD) is manifested through loss of memory, disorientation, and difficulty performing daily tasks. AD is a growing epidemic, affecting more than 25 million people worldwide.[1] A hallmark of AD is insoluble extracellular senile plaques composed of a 39−42 residue peptide fragment termed amyloid-β (Aβ). Aβ is generated during normal cleavage of the membrane-anchored amyloid precursor protein (APP) by β- and γ-secretases.[2] Roughly one-third of the Aβ owes its high degree of insolubility to the fact that 12−14 of its residues derive from the membrane-anchoring C-terminal region of the parent APP protein.[3] Studies have shown that Aβ interacts with and aggregates at membrane surfaces, presumably because of its amphiphilic nature.[4−10] Yet, the mechanism of these membrane-induced aggregation events are not well understood.

Protein−lipid interactions are diverse and can cause dramatic structural changes in proteins, resulting in folding, unfolding, or even misfolding. For example, human islet amyloid polypeptide (hIAPP or amylin), associated with type II diabetes, forms β-sheet aggregates in the presence of anionic lipids.[11] Conversely, the naturally occurring prion protein (PrP_C), normally associated with cholesterol-rich lipid rafts,[12] may translocate to lipid domains with altered levels of cellular cholesterol and convert to the misfolded form (PrP_{Sc}).[13] Aβ is a complex peptide, demonstrating structural plasticity depending on the preparation and incubation time. In aqueous solvents, Aβ is disordered in its monomeric form[14] and is β-sheet structured in its fibrillar form.[15] Aβ begins to form oligomeric structures within the first 24−48 h of incubation at 37 °C.[9] These oligomeric species come in many forms, including amlyloid-derived diffusible ligands (ADDL's),[16] protofibrils,[17] annular protofibrils,[18] and globulomers.[19] Although the tertiary structure of early oligomers, protofibrils, and globulomers are vastly different, they all have β-sheet secondary structure.[17,19,20] However, studies of Aβ(1−40) in SDS micelles indicate the formation of stable α-helical structure above the critical micelle concentration.[21] NMR studies have localized the α-helical structure of Aβ(1−40) to residues 15−24 and 29−35, with a kink at residues 25−28.[22,23] Other studies indicate the potential of ion channels or a β-sheet-structured pore in lipid membranes.[24−26] Aβ has also been shown to undergo α-helical to β-sheet conformational changes in the presence of low concentrations of fluorinated alcohols.[14] Mounting evidence suggests that the increased neurotoxicity of Aβ oligomers is derived from their interactions with neuronal membranes.[27]

It is currently known that disordered Aβ binds to model membranes and forms α-helical and β-sheet structures depending on the lipid characteristics,[5] whereas oligomers may bind model membranes and form pore-like structures.[26]

Received: December 5, 2013
Revised: March 31, 2014
Published: April 4, 2014

Although the instability of Aβ's structure in membrane-mimicking environments is known, a better understanding of how membrane characteristics affect the binding, solvation, and secondary structure of Aβ is still needed.

Deep-UV resonance Raman (dUVRR) spectroscopy has been employed to study oligomerization and amyloid fibril formation in the aqueous environment.[28] Furthermore, comparative dUVRR studies, using 197 nm excitation on predominantly α-helical proteins, show that transmembrane (TM) proteins have an unusually strong amide I band.[29,30] In fact, the amide I mode appears to be highly sensitive to solvent-mediated hydrogen bonding, or lack thereof, consistent with its enhancement in lipid environments,[31,32] making it a logical tool for localization of the transient structure versus the membrane proper. Therefore, dUVRR analysis was utilized to understand better how lipid membranes and bilayer content affect the structures of Aβ and how these ensemble structures change over time.

EXPERIMENTAL PROCEDURES

Crude Aβ(25−40) and Aβ(1−40) peptides were synthesized by the Structural Biology Core Facility, University of Missouri−Columbia, and were further purified using an analytical System Gold HPLC (Beckman Coulter, Brea, CA) fitted with a C18 column (Grace Vydac protein and peptide, Deerfield, IL). Acetonitrile (Fisher Scientific, Pittsburgh, PA) and water (pH 2.5) were employed to optimize separation. $AcWL_5$ was purchased from Pi Proteomics (Huntsville, AL) and used without further purification. DMPC, DMPG, DLPG, and DDPG lipid powder were obtained from Avanti Polar Lipids (Alabaster, AL). DMPG was dissolved in a mixture of chloroform (Fisher Scientific, Pittsburgh, PA)/methanol (Fisher Scientific, Pittsburgh, PA)/water (65:35:8, v/v/v). DMPC, DLPG, and DDPG were dissolved in extra-dry chloroform (Acros Organics, Geel, Belgium). Lipid solutions were transferred into glass test tubes, dried under argon, and kept under vacuum overnight to remove any trace of solvent. Phosphate buffer was prepared using monobasic sodium phosphate, dibasic sodium phosphate, sodium chloride (Fisher Scientific, Pittsburgh, PA), and sodium perchlorate (Sigma, St. Louis, MO). For sample preparation, approximately 1.5 mg of purified Aβ(25−40) in 10 mM sodium phosphate buffer, pH 7.4, was sonicated at 4 °C for 2 min to break up aggregates. Any remaining insoluble aggregates were removed by centrifugation for 30 min at 14 000 rcf at 4 °C. The concentration of the Aβ(25−40) solution was estimated using a molar extinction coefficient of 17 385 M^{-1} cm^{-1}, which was estimated from the side chain and peptide bond extinction coefficients at 215 nm.[33] Aβ(1−40) was prepared similarly except that the concentration was determined using the tyrosine molar extinction coefficient of 1405 M^{-1} cm^{-1} at 274 nm. The concentration was adjusted to 50 μM for aqueous samples. The lipids were resuspended in 20 mM phosphate buffer, pH 7.4, with 5 mM NaCl and sonicated at 50 °C for 1 h. The solution was then extruded with a 100 nm pore diameter polycarbonate membrane (Avestin Inc., Ottawa, Canada) to produce monodisperse liposomes. The concentration of the lipids was then estimated by a Rouser assay,[34] and the size distribution of the liposomes was determined using a DynaPro-MSTC dynamic light scattering (DLS) instrument (Protein Solution Inc., Somerset, NJ). Lastly, the peptide solution was added to the concentrated liposome solution at a 1:100 peptide/lipid ratio for a final concentration of 50 μM peptide and 5 mM lipid. The $AcWL_5$ peptide was hydrated with 15 mM DMPC lipid and incubated at 37 °C for at least 4 h. The peptide concentration of 0.13 mM was determined by the tryptophan absorbance at 280 nm with an extinction coefficient of 5560 M^{-1} cm^{-1}. Then, the insertion of $AcWL_5$ was confirmed by fluorescence using a Cary Eclipse fluorometer (Varian, Palo Alto, CA). A shift in the tryptophan fluorescence maximum from 345 nm in an aqueous solution to 335 nm in a lipid environment is expected.[35] Poly-L-lysine was dissolved in 10 mM phosphate buffer, pH 7.00, for a final concentration of 24 μM. The pH was then increased to 11.40 using NaOH (Fisher Scientific, Pittsburgh, PA). The poly-L-lysine solution was then heated at 55 °C to produce β-sheet structure.

Deep-Ultraviolet Resonance Raman Spectroscopy. The dUVRR system and those similar have been described elsewhere.[33,36] An excitation wavelength of 197 nm was generated from the fourth harmonic of a Ti:sapphire laser pumped by a Nd:YLF laser system (Coherent Inc., Santa Clara, CA). Samples were held in a custom-made water-jacketed reservoir (Mid Rivers Glassblowing, St. Charles, MO) under nitrogen gas and circulated through a pair of nitinol wires by a Minipuls2 peristaltic pump (Gilson Inc., Middleton, WI) to generate a thin film of sample. The laser power at the sample was kept at less than 500 μW to prevent photodegradation. The Raman signal was collected by a Symphony CCD camera (Horiba Jobin Yvon Inc., Edison, NJ) with a chip size of 2048 × 512. A bin of 4 was applied in the horizontal direction for a final resolution of approximately 2.4 cm^{-1}. Each spectrum was collected for 6 h and exported using Synergy software (Horiba Jobin Yvon Inc., Edison, NJ). A small aliquot of a 1 M sodium perchlorate solution was added to each sample, for a final concentration of 50 mM, as an internal intensity standard. All spectra were calibrated using a standard cyclohexane spectrum.

Circular Dichroism Spectroscopy. All samples used for dUVRR analysis were additionally measured for their corresponding CD spectra. An AVIV 62DS circular dichroism (Aviv Biomedical Inc., Lakewood Township, NJ) spectrometer and a quartz cell with a 1 mm optical path length (Hellma USA, Plainview, NY) were used to collect CD spectra. All spectra were collected between 190 and 250 nm with a resolution of 0.1 nm at room temperature. Every sample was measured five times with a scan speed of 1 nm/5 s. Corresponding background spectra were collected in the same manner and subtracted from sample spectra.

Data Analysis. All spectra were analyzed in the Matlab (Mathworks, Natick, MA) environment. Mean residue molar ellipticity (θ_{MRE}) was calculated as previously described,[33] and the spectra were fit with mixed Gaussian/Lorentzian bands. All dUVRR data were preprocessed using a custom cosmic spike removal tool, and buffer contributions were removed from averaged and baseline-corrected spectra according to methods described elsewhere.[37]

RESULTS

Aβ(25−40) contains the hydrophobic region of full-length Aβ(1−40), which is part of the TM domain of APP. To determine if Aβ(25−40) could form a stable structure in the presence of membrane-mimicking environments, CD and dUVRR spectra were recorded in the presence of neutral DMPC and anionic DMPG liposomes.

Environmental Dependence of Aβ(25−40)'s Structure. Previous studies of the structure of Aβ(25−40) in aqueous environments indicate that the peptide adopts a disordered

dx.doi.org/10.1021/bi4016296 | Biochemistry 2014, 53, 3004−3011

structure.[20,33] The CD spectra of Aβ(25−40) have a strong negative feature at 197 nm and a weak negative feature at 220 nm, indicative of a predominantly disordered structure with a small amount of β-strand structure (Figure 1). Similarly, the

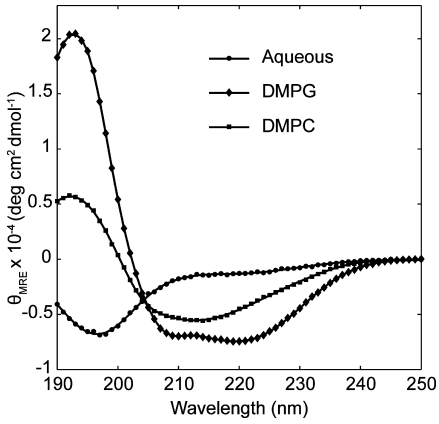

Figure 1. CD spectra of Aβ(25−40) in aqueous buffer (●), DMPG (♦) and DMPC (■).

dUVRR spectrum of the aqueous peptide is also consistent with a disordered structure, as revealed by the amide I, S, and III bands at 1656, 1387, and 1249/1300 cm^{-1}, respectively (Figure 2).[38]

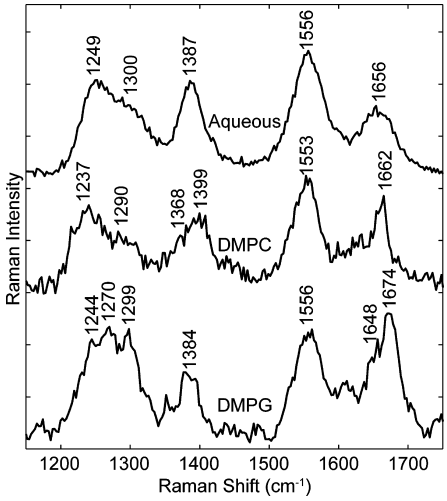

Figure 2. dUVRR spectra of Aβ(25−40) in aqueous buffer (top), DMPC (middle), and DMPG (bottom).

Although it is thought that interactions with the membrane surface will cause β-sheet and aggregate formation, less is known about the structural consequences arising from this equilibration. In the presence of neutrally charged lipid bilayers (DMPC), Aβ(25−40) forms β-sheet structure very quickly. Specifically, the CD spectrum of Aβ(25−40) in solution with DMPC liposomes has a positive feature at 193 nm and a negative feature at 213 nm, which is consistent with β-sheet structure,[39] whereas the dUVRR spectrum has a narrow amide I band located at 1662 cm^{-1}, an asymmetrical amide S feature at 1399 cm^{-1}, and an amide III region that can be deconvoluted into two features at 1237 and 1290 cm^{-1}. The first amide III feature, sometimes referred to as the amide III$_3$ mode,[40,41] is dependent on the ψ dihedral angle, and a Raman shift of 1237 cm^{-1} is most consistent with β-sheet structure.

Association of Aβ(25−40) with negatively charged liposomes (DMPG) has a significantly different influence on the secondary structures adpoted by this hydrophobic peptide. In fact, the CD spectrum of Aβ(25−40), with a positive feature at 193 nm and two negative features at 209 and 221 nm, is consistent with classical α-helical structure. In contrast, the dUVRR spectrum of the sample contains an amide III band contribution at 1244 cm^{-1} and a significant amide S band at 1384 cm^{-1} in addition to contributions at the α-helical-correlated positions (1270/1299 cm^{-1}), suggesting that the peptide contains both helical and nonhelical structures (Figure 2).[42] Interestingly, the amide I mode of Aβ(25−40) in DMPG is stronger in intensity than the amide II band and is best fit with two peaks centered at 1648 and 1674 cm^{-1}. The first component at 1648 cm^{-1} is consistent with dehydrated helical structure,[43,44] whereas the second component is consistent with β-sheet structure. Previous studies have shown that the intensity of the amide I mode in dUVRR spectra is an intrinsic marker for membrane association,[29,30] and the increase in its intensity has been attributed to desolvation of the peptide backbone in membrane environments. Therefore, some portion of the Aβ(25−40) backbone is likely hidden from water by the membrane.

Although the first amide I feature at 1648 cm^{-1} is characteristic of helical structure, the second feature at 1674 cm^{-1} is higher than would be expected for disordered structure, but it might be attributable to β-sheet structure. However, there have been only a limited number of dUVRR studies on β-sheet-structured membrane proteins;[45] therefore, to aid in assigning the second amide I feature, a simple hydrophobic peptide, AcWL$_5$, reported previously to assemble into a transmembrane β-sheet when exposed to a lipid bilayer environment,[45,46] was examined. dUVRR studies conducted on AcWL$_5$ in the presence of DMPC liposomes confirm that AcWL$_5$ is associated with the membrane because of the similarly intense amide I mode versus that of the soluble β-sheet-structured poly-L-lysine at high pH and temperature (Figure 3). The amide I region of AcWL$_5$ can be fit by a single narrow band centered at 1675 cm^{-1}, which directly overlaps with the amide I band in the β-sheet poly-L-lysine spectrum. Amide III (1245 cm^{-1}) and amide S (1400 cm^{-1}) band positions confirm that AcWL$_5$ adopts β-sheet structure and indicate that the intense amide I position at

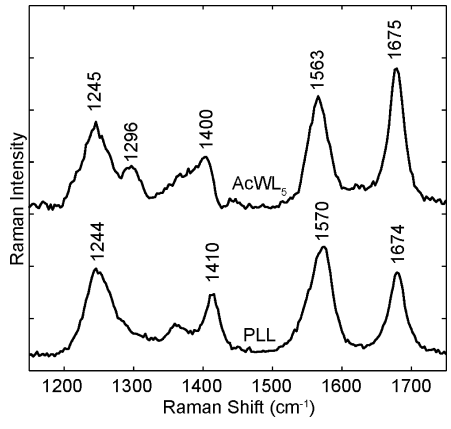

Figure 3. dUVRR spectra of AcWL$_5$ (top, TM β-sheet structure) and poly-L-lysine (bottom, soluble β-sheet structure).

dx.doi.org/10.1021/bi4016296 | *Biochemistry* 2014, 53, 3004−3011

1675 cm^{-1} in the dUVRR spectrum of Aβ(25−40) in DMPG is likely derived from β-sheet structural content.

Dependence of Aβ(25−40) Structure on Hydrophobic Thickness. Because Aβ(25−40) adopts a mixture of helical and β-sheet structures and because some portion of this peptide appears to be buried in the membrane interior when it is exposed to anionic DMPG lipid bilayers, assessment of the influence of hydrophobic thickness on the lipid equilibrated peptide structure is necessary. CD and dUVRR spectra of Aβ(25−40) were collected in the presence of DLPG and DDPG, which have hydrophobic thicknesses of 19.0 and 16.5 Å, respectively. The CD spectrum of Aβ(25−40) in DLPG, dominated by a single positive feature at 192 nm and two negative features at 205 and 223 nm, indicates that the peptide adopts a mixture of α-helical and disordered structure (Figure 4). The loss of intensity at 223 nm when comparing the CD

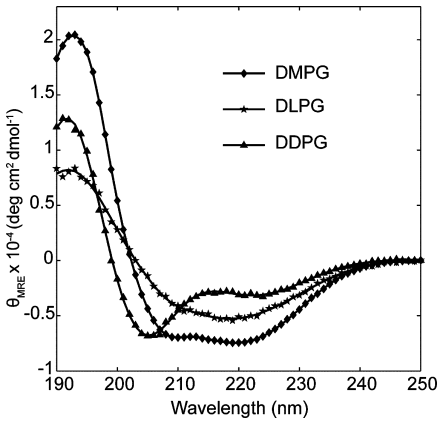

Figure 4. CD spectra of Aβ (25−40) with DMPG (♦), DLPG (★), and DDPG (▲).

spectrum of Aβ(25−40) with DLPG versus DMPG suggests a decrease in the peptide's helical content when equilibrating with thinner lipid bilayers. The corresponding dUVRR spectrum is consistent with an increase of nonhelical content (Figure 5), as the amide S mode (1388 cm^{-1}) is stronger in the dUVRR spectrum of Aβ(25−40) interacting with DLPG versus

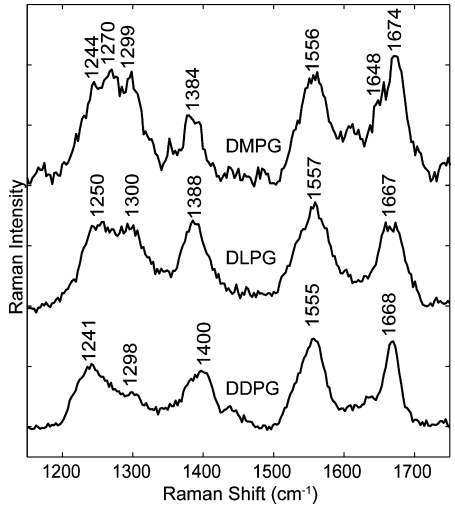

Figure 5. dUVRR spectra of Aβ(25−40) with DMPG (top), DLPG (middle), and DDPG (bottom).

DMPG bilayers. Furthermore, the position of the lowest-frequency band in the amide III region occurs at 1250 cm^{-1}, which is characteristic of disordered structure, whereas the second easily resolved feature in the amide III region at 1300 cm^{-1} is more consistent with α-helical structural content.

In contrast to other anionic lipids and similar to the neutral DMPC membrane interactions, the negative feature at 219 nm and the positive feature at 193 nm (Figure 4) in the CD spectrum as well as the amide III, S, and I bands at 1241, 1400, and 1668 cm^{-1} in the dUVRR spectrum (Figure 5) suggest a predominantly β-sheet-structured peptide. These findings suggest that the thickness of the bilayer will influence the equilibration of the peptide with and within the membrane.

Structural Transition of Aβ(25−40) in DLPG over Time. Because Aβ(25−40) equilibrates with anionic membranes and undergoes a structural transition in the presence of a membrane environment, the equilibration of the peptide's structure over time is of interest to understand how these membranes may or may not facilitate the formation of β-sheet-comprised fibrillar aggregates. Given that the transition temperature of DMPG is near room temperature and that Aβ(25−40) appears not to equilibrate with or into DDPG lipid bilayers, the CD spectrum of Aβ(25−40) in DLPG liposomes, containing a mixture of α-helical and disordered structure, was monitored over time. Within the first 48 h of incubation at room temperature, the positive feature at 193 nm increases, concurrent with a decrease of the negative feature at 205 nm, indicating a loss of disordered structure (Figure 6). However, β-

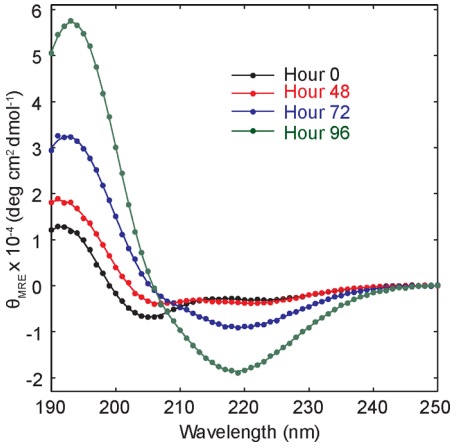

Figure 6. CD spectra of Aβ (25−40) with DLPG incubated over 96 h at rt.

sheet structure does not appear to contribute significantly to the CD spectrum until after 72 h of incubation. After 96 h of incubation, the peptide contains a significant amount of β-sheet structure, as shown by a strong negative feature at 219 nm. The lack of an isosbestic point indicates that this process is not a two-state transition.

Structural Transition of Aβ(1−40) in DLPG over Time. Aβ(25−40) contains only the hydrophobic portion of the full-length peptide, Aβ(1−40). Previous studies have shown that the full-length peptide also interacts with membranes.[47] However, whether the hydrophobic region will interact in a similar manner with anionic membranes when a significant water-soluble portion is also present remains to be tested.

Both CD and dUVRR spectra of Aβ(1−42) in aqueous solution have been reported previously[20] and should be similar

dx.doi.org/10.1021/bi4016296 | *Biochemistry* 2014, 53, 3004−3011

to Aβ(1−40) in its monomeric form.[20,28,33] In the presence of DLPG liposomes, two minima located at 207 and 222 nm in the CD spectra indicate that Aβ(1−40) also adopts a mixture of disordered and helical structure (Figure 7), which is similar to

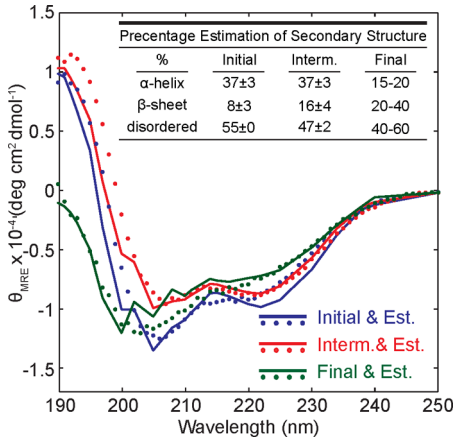

Figure 7. Initial (blue), intermediate (red), and final (green) CD spectra of Aβ(1−40) with DLPG with simulations (dotted lines and inset table).

Aβ(25−40). To estimate the conformational changes in Aβ(1−40) over time better, CD spectra were fit using CD spectra derived from poly-L-lysine in its α-helical, β-sheet, and disordered conformations.[48] Three replicates of Aβ(1−40) in DLPG spectra were analyzed in this manner (Figure 7, inset). These analyses suggest that the peptide gradually loses disordered character in favor of a small amount of β-sheet structure after 48 h of incubation at room temperature (Figure 7, intermediate). Longer incubation times result in an overall loss of helical structure in favor of β-sheet and disordered structure based on the fitted spectra. In each case, the final conformational ensemble is variable; therefore, ranges are given in the inset table (Figure 7), and the mean for each is reported (Table 1). The spectrum after 9 days of incubation shows that the minimum at 205 nm has shifted to 202 nm. The maximum at 193 nm is also less-intense, consistent with an increase in disordered structure. A decrease in the intensity of the minimum at 222 nm is consistent with a loss of helical structure.

The dUVRR spectrum of Aβ(1−40) prior to lipid addition is consistent with the peptide having a disordered conformation, as evidenced by the amide I (1669 cm^{-1}), II (1557 cm^{-1}), S (1393 cm^{-1}), and III (1252 and 1297 cm^{-1}) band positions (Figure 8, aqueous). The bands at 1211 and 1608 cm^{-1} are derived from both the phenylalanine and tyrosine residues, which are absent in Aβ(25−40). Phenylalanine also has a strong band located at 1002 cm^{-1} (not shown in figure). Overall, the intensity of the aromatic modes increases upon transition from an aqueous to a lipid environment. The initial spectrum of Aβ(1−40) interacting with DLPG liposomes

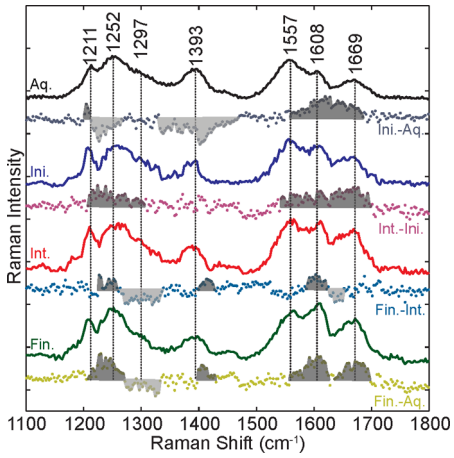

Figure 8. dUVRR spectra of Aβ(1−40) in water (black) and initial (blue), intermediate (red), and final (green) with DLPG. The dotted lines are difference spectra of initial − water (blue dots), intermediate − initial (red dots), final − intermediate (green dots), and final − water (yellow dots).

(Figure 8, initial) shows that some portion the full-length Aβ peptide has characteristics consistent with burial of the peptide backbone in the membrane, as indicated by the enhanced amide I band at 1663 cm^{-1} and the increased intensity of the aromatic modes (Figure 8, top difference spectrum). Increases in the amide mode intensities could be attributed to an α-helical to β-sheet or disordered conformation transition or, conversely, to a disordered to β-sheet conformation transition. The final dUVRR spectrum of Aβ(1−40) after 9 days of incubation in DLPG shows a loss of intensity at 1330 cm^{-1}, consistent with a loss of α-helical structure. An increase in the intensity of the amide III band at 1240 cm^{-1} along with an increase in the amide S intensity is also consistent with an increase in β-sheet structure, indicting the latter pathway is the most likely. Table 2 summarizes the fitted amide mode positions for both Aβ(25−40) and Aβ(1−40).

DISCUSSION

Previous studies have shown that the dramatically enhanced amide I band is a unique marker for desolvation of the peptide backbone, which can result from cross-β-sheet core formation in amyloid fibrils or can be driven by the insertion of the peptide into a lipid environment.[29,30] Because the amide I band intensity increases with the introduction of anionic lipids, but is not directly correlated with β-sheet formation, some portion of the Aβ(25−40) is likely buried in the anionic bilayer. Although the initial CD spectrum of Aβ(25−40) in DMPG indicates the existence of a large percentage of α-helix initially, the dUVRR spectrum of the same sample provides more detailed information. A typical α-helical dUVRR spectrum should have three features within the amide III region: 1276, 1293, and 1339 cm^{-1}. A pure α-helix should also lack an amide S

Table 1. Summary of Structural Estimation for Aβ(25−40) and Aβ(1−40) with Liposomes

	Aβ(25−40)				Aβ(1−40) with DLPG		
%	DMPC	DMPG	DLPG	DDPG	initial	intermediate	final
α-helix	15	75	40	24	37	37	17
β-sheet	55	15	10	53	8	16	30
disordered	30	10	50	23	55	47	53

dx.doi.org/10.1021/bi4016296 | Biochemistry 2014, 53, 3004−3011

Table 2. Summary of Raman Shifts (cm^{-1}) for Aβ(25−40) and Aβ(1−40) with Liposomes

	Aβ(25−40)				Aβ(1−40) with DLPG		
	DMPC	DMPG	DLPG	DDPG	initial	intermediate	final
	1237	1244	1250	1241	1243	1242	1252
amide III	1290	1270	1300	1298	1273	1270	1297
		1299			1304	1298	
amide S	1399	1384	1388	1400	1386	1388	1393
amide II	1553	1556	1557	1555	1559	1560	1557
amide I	1662	1674	1667	1668	1663	1667	1669

feature, as this mode is disallowed in nonhelical conformations.[49] The spectrum of Aβ(25−40) in DMPG has a relatively strong amide S feature, and the amide III 1244 cm^{-1} feature is likely derived from nonhelical secondary structure. These results are not surprising because the lysine residue near the N-terminus of the Aβ(25−40) peptide provides a significant barrier to the full insertion of the peptide into the bilayer environment.

Because the equilibration of Aβ(25−40) is heavily influenced by bilayer thickness, hydrophobic mismatch is a potential cause of the structural complexity of Aβ(25−40) in a lipid environment. Hydrophobic mismatch, when the protein structure is longer or shorter than the length of the lipid bilayer, may cause structural instability of TM peptides. The hydrophobic thickness of DMPG is estimated to be 23.5 Å. Assuming that all 29−40 residues are embedded in the membrane and folded into a helical conformation, the length of the helix would only be 18.0 Å, leading to hydrophobic mismatch. To fit the DMPG liposome, Aβ(25−40) may form extended helices so that the peptide can span the bilayer, which is consistent with the lack of the characteristic 1300 and 1330 cm^{-1} features in the amide III-affiliated spectral region. Membrane thinning may also occur near the peptide because of lipid rearrangements, leading to the mixed secondary structure described earlier. DLPG has a hydrophobic thickness of 19.0 Å, which best fits the hydrophobic portion of the peptide but leaves the N-terminus residues outside the hydrophobic interior, resulting in the disordered structure identified by both CD and UVRR. The DDPG liposomes provide the thinnest hydrophobic region at 16.5 Å while also having the most extreme curvature of any of the liposomes. Thus, it is plausible that DDPG cannot accommodate the peptide and that the hydrophobic portion of the peptide becomes exposed to the aqueous environment and folds into β-sheet structure.

Full-length Aβ(1−40) is much more amphiphilic than the smaller Aβ(25−40) peptide fragment, as it contains significant hydrophobic and hydrophilic regions. On the basis of the initial, intermediate, and final CD and dUVRR spectra of Aβ(1−40), a model of the structural transition of the peptide is proposed (Figure 9). The initial stage contains a liposome-embedded α-helix formed by the C-terminus of Aβ(1−40), whereas the N-terminus remains disordered and is exposed to the aqueous environment. The ordering parameters associated with the interactions of the peptide with the anionic lipid bilayer surface drives the transition to more folded structures,[50] which, in this case, is β-sheet structure at the N-terminus, whereas the C-terminus α-helix remains relatively stable initially. Lastly, as the stability of the β-sheet structure takes hold, the α-helix, presumably held together by lateral forces of the membrane acyl chains, is disrupted and begins to unfold and come out of the membrane.

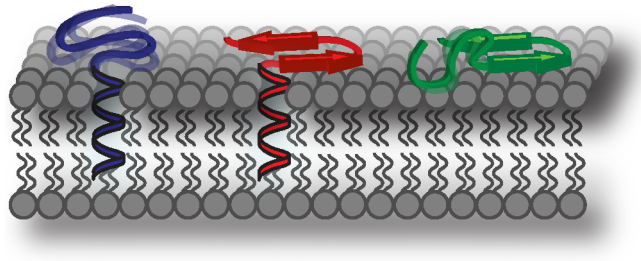

Figure 9. Model of Aβ(1−40) interacting with DLPG liposomes via three stages: initial (blue), intermediate (red), and final (green).

It is enticing to hypothesize that this in vitro-derived scenario may mimic the process by which the newly cleaved Aβ peptide emerges from the lipid bilayer. If this is, in fact, the case, then this would represent the first experimentally derived model for how Aβ sheet formation may occur initially.

AUTHOR INFORMATION

Corresponding Author

*Phone: 573-882-8949; Fax: 573-882-2754; E-mail: JiJiR@missouri.edu.

Funding

This research was supported by an NSF CAREER award (CHE-1151533) and the University of Missouri−Columbia.

Notes

The authors declare no competing financial interest.

ACKNOWLEDGMENTS

We acknowledge the Structural Biology Core Facility, University of Missouri−Columbia, for the use of the DLS instrument. We also thank Dr. Fabio Gallazzi, Structural Biology Core Facility, University of Missouri−Columbia, for peptide synthesis and Dr. Michael Henzl, Department of Biochemistry, University of Missouri−Columbia, for the help with CD measurements.

ABBREVIATIONS USED

Aβ peptide, β-amyloid peptide; dUVRR, deep-UV resonance Raman; TM, transmembrane; APP, amyloid precursor protein; CD, circular dichroism; HPLC, high-performance liquid chromatography; DMPC, 1,2-dimyristoyl-*sn*-glycero-3-phosphocholine; DMPG, 1,2-ditetradecanoyl-*sn*-glycero-3-phospho-(1′-*rac*-glycerol); DLPG, 1,2-didodecanoyl-*sn*-glycero-3-phospho-(1′-*rac*-glycerol); DDPG, 1,2-didecanoyl-*sn*-glycero-3-phospho-(1′-*rac*-glycerol); DLS, dynamic light scattering

REFERENCES

(1) O'Brien, R. J., and Wong, P. C. (2011) Amyloid precursor protein processing and Alzheimer's disease. *Annu. Rev. Neurosci. 34*, 185−204.

(2) Haass, C., and Selkoe, D. J. (2007) Soluble protein oligomers in neurodegeneration: Lessons from the Alzheimer's amyloid β-peptide. *Nat. Rev. Mol. Cell Biol. 8*, 101−112.
(3) Barrett, P. J., Song, Y., Van Horn, W. D., Hustedt, E. J., Schafer, J. M., Hadziselimovic, A., Beel, A. J., and Sanders, C. R. (2012) The amyloid precursor protein has a flexible transmembrane domain and binds cholesterol. *Science 336*, 1168−1171.
(4) Bokvist, M., and Gröbner, G. (2007) Misfolding of amyloidogenic proteins at membrane surfaces: The impact of macromolecular crowding. *J. Am. Chem. Soc. 129*, 14848−14849.
(5) Bokvist, M., Lindström, F., Watts, A., and Gröbner, G. (2004) Two types of Alzheimer's β-amyloid (1−40) peptide membrane interactions: Aggregation preventing transmembrane anchoring versus accelerated surface fibril formation. *J. Mol. Biol. 335*, 1039−1049.
(6) Byström, R., Aisenbrey, C., Borowik, T., Bokvist, M., Lindström, F., Sani, M.-A., Olofsson, A., and Gröbner, G. (2008) Disordered proteins: Biological membranes as two-dimensional aggregation matrices. *Cell Biochem. Biophys. 52*, 175−189.
(7) de Planque, M. R. R., Raussens, V., Contera, S. A., Rijkers, D. T. S., Liskamp, R. M. J., Ruysschaert, J.-M., Ryan, J. F., Separovic, F., and Watts, A. (2007) β-Sheet structured β-amyloid(1−40) perturbs phosphatidylcholine model membranes. *J. Mol. Biol. 368*, 982−997.
(8) Kawahara, M., Ohtsuka, I., Yokoyama, S., Kato-Negishi, M., and Sadakane, Y. (2011) Membrane incorporation, channel formation, and disruption of calcium homeostasis by Alzheimer's β-amyloid protein. *Int. J. Alzheimer's Dis.*, 1−17.
(9) Kayed, R., Head, E., Thompson, J. L., McIntire, T. M., Milton, S. C., Cotman, C. W., and Glabe, C. G. (2003) Common structure of soluble amyloid oligomers implies common mechanism of pathogenesis. *Science 300*, 486−489.
(10) Terzi, E., Hölzemann, G., and Seelig, J. (1997) Interaction of Alzheimer β-amyloid peptide(1−40) with lipid membranes. *Biochemistry 36*, 14845−14852.
(11) Xiao, D., Fu, L., Liu, J., Batista, V. S., and Yan, E. C. Y. (2012) Amphiphilic adsorption of human islet amyloid polypeptide aggregates to lipid/aqueous interfaces. *J. Mol. Biol. 421*, 537−547.
(12) Taylor, D. R., and Hooper, N. M. (2006) The prion protein and lipid rafts (Review). *Mol. Membr. Biol. 23*, 89−99.
(13) Jeong, J.-K., M, M.-H., Lee, Y.-J., Seol, J.-W., and Park, S.-Y. (2012) Translocation of cellular prion protein to non-lipid rafts protects human prion-mediated neuronal damage. *Int. J. Mol. Med. 29*, 387−292.
(14) Barrow, C. J., Yasuda, A., Kenny, P. T. M., and Zagorski, M. G. (1992) Solution conformations and aggregational properties of synthetic amyloid β-peptides of Alzheimer's disease: Analysis of circular dichroism spectra. *J. Mol. Biol. 225*, 1075−1093.
(15) Tycko, R. (2011) Solid-state NMR studies of amyloid fibril structure. *Annu. Rev. Phys. Chem. 62*, 279−299.
(16) Lambert, M. P., Barlow, A. K., Chromy, B. A., Edwards, C., Freed, R., Liosatos, M., Morgan, T. E., Rozovsky, I., Trommer, B., Viola, K. L., Wals, P., Zhang, C., Finch, C. E., Krafft, G. A., and Klein, W. L. (1998) Diffusible, nonfibrillar ligands derived from Aβ1−42 are potent central nervous system neurotoxins. *Proc. Natl. Acad. Sci. U.S.A. 95*, 6448−6453.
(17) Walsh, D. M., Hartley, D. M., Kusumoto, Y., Fezoui, Y., Condron, M. M., Lomakin, A., Benedek, G. B., Selkoe, D. J., and Teplow, D. B. (1999) Amyloid β-protein fibrillogenesis: Structure and biological activity of protofibrillar intermediates. *J. Biol. Chem. 274*, 25945−25952.
(18) Kayed, R., Pensalfini, A., Margol, L., Sokolov, Y., Sarsoza, F., Head, E., Hall, J., and Glabe, C. (2009) Annular protofibrils are a structurally and functionally distinct type of amyloid oligomer. *J. Biol. Chem. 284*, 4230−4237.
(19) Yu, L., Edalji, R., Harlan, J. E., Holzman, T. F., Lopez, A. P., Labkovsky, B., Hillen, H., Barghorn, S., Ebert, U., Richardson, P. L., Miesbauer, L., Solomon, L., Bartley, D., Walter, K., Johnson, R. W., Hajduk, P. J., and Olejniczak, E. T. (2009) Structural characterization of a soluble amyloid β-peptide oligomer. *Biochemistry 48*, 1870−1877.
(20) Wang, M., and JiJi, R. D. (2011) Spectroscopic detection of β-sheet structure in nascent Aβ oligomers. *J. Biophotonics 4*, 637−644.
(21) Rangachari, V., Reed, D. K., Moore, B. D., and Rosenberry, T. L. (2006) Secondary structure and interfacial aggregation of amyloid-β(1−40) on sodium dodecyl sulfate micelles. *Biochemistry 45*, 8639−8648.
(22) Coles, M., Bicknell, W., Watson, A. A., Fairlie, D. P., and Craik, D. J. (1998) Solution structure of amyloid β-peptide(1−40) in a water−micelle environment. Is the membrane-spanning domain where we think it is? *Biochemistry 37*, 11064−11077.
(23) Jarvet, J., Danielsson, J., Damberg, P., Oleszczuk, M., and Gräslund, A. (2007) Positioning of the Alzheimer Aβ(1−40) peptide in SDS micelles using NMR and paramagnetic probes. *J. Biomol NMR 39*, 63−72.
(24) Micelli, S., Meleleo, D., Picciarelli, V., and Gallucci, E. (2004) Effect of sterols on β-amyloid peptide (AβP 1−40) channel formation and their properties in planar lipid membranes. *Biophys. J. 86*, 2231−2237.
(25) Alarcón, J. M., Brito, J. A., Hermosilla, T., Atwater, I., Mears, D., and Rojas, E. (2006) Ion channel formation by Alzheimer's disease amyloid β-peptide (Aβ40) in unilamellar liposomes is determined by anionic phospholipids. *Peptides 27*, 95−104.
(26) Jang, H., Arce, F. T., Ramachandran, S., Capone, R., Lal, R., and Nussinov, R. (2010) β-Barrel topology of Alzheimer's β-amyloid ion channels. *J. Mol. Biol. 404*, 917−934.
(27) Hardy, J., and Selkoe, D. J. (2002) The amyloid hypothesis of Alzheimer's disease: Progress and problems on the road to therapeutics. *Science 297*, 353−356.
(28) Popova, L. A., Kodali, R., Wetzel, R., and Lednev, I. K. (2010) Structural variations in the cross-β core of amyloid β fibrils revealed by deep UV resonance Raman sSpectroscopy. *J. Am. Chem. Soc. 132*, 6324−6328.
(29) Halsey, C. M., Oshokoya, O. O., Jiji, R. D., and Cooley, J. W. (2011) Deep-UV resonance Raman analysis of the *Rhodobacter capsulatus* cytochrome bc1 complex reveals a potential marker for the transmembrane peptide backbone. *Biochemistry 50*, 6531−6538.
(30) Halsey, C. M., Xiong, J., Oshokoya, O. O., Johnson, J. A., Shinde, S., Beatty, J. T., Ghirlanda, G., JiJi, R. D., and Cooley, J. W. (2011) Simultaneous observation of peptide backbone lipid solvation and α-helical structure by deep-UV resonance Raman spectroscopy. *ChemBioChem. 12*, 2125−2128.
(31) Ozdemir, A., Lednev, I. K., and Asher, S. A. (2005) UVRR spectroscopic studies of valinomycin complex formation in different solvents. *Spectrochim. Acta, Part A 61*, 19−26.
(32) Wang, Y., Purrello, R., Georgiou, S., and Spiro, T. G. (1991) UVRR spectroscopy of the peptide bond. 2. Carbonyl H-bond effects on the ground- and excited-state structures of N-methylacetamide. *J. Am. Chem. Soc. 113*, 6368−6377.
(33) Wang, M., and JiJi, R. D. (2011) Resolution of localized small molecule−Aβ interactions by deep-ultraviolet resonance Raman spectroscopy. *Biophys. Chem. 158*, 96−103.
(34) Rouser, G., Fleischer, S., and Yamamoto, A. (1970) Two dimensional thin layer chromatographic separation of polar lipids and determination of phospholipids by phosphorus analysis of spots. *Lipids 5*, 494−496.
(35) Ladokhin, A. S., Jayasinghe, S., and White, S. H. (2000) How to measure and analyze tryptophan fluorescence in membranes properly, and why bother? *Anal. Biochem. 285*, 235−245.
(36) Balakrishnan, G., Hu, Y., Nielsen, S. B., and Spiro, T. G. (2005) Tunable kHz deep ultraviolet (193−210 nm) laser for Raman application. *Appl. Spectrosc. 59*, 776−781.
(37) Simpson, J. V., Balakrishnan, G., and JiJi, R. D. (2009) MCR-ALS analysis of two-way UV resonance Raman spectra to resolve discrete protein secondary structural motifs. *Analyst 134*, 138−147.
(38) Huang, C.-Y., Balakrishnan, G., and Spiro, T. G. (2006) Protein secondary structure from deep-UV resonance Raman spectroscopy. *J. Raman Spectrosc. 37*, 277−282.
(39) Danielsson, J., Jarvet, J., Damberg, P., and Gräslund, A. (2005) The Alzheimer β-peptide shows temperature-dependent transitions

between left-handed 31-helix, β-strand and random coil secondary structures. *FEBS J. 272*, 3938−3949.
(40) Mikhonin, A. V., Bykov, S. V., Myshakina, N. S., and Asher, S. A. (2006) Peptide secondary structure folding reaction coordinate: Correlation between UV Raman amide III frequency, Ψ Ramachandran angle, and hydrogen bonding. *J. Phys. Chem. B 110*, 1928−1943.
(41) Oladepo, S. A., Xiong, K., Hong, Z., Asher, S. A., Handen, J., and Lednev, I. K. (2012) UV resonance Raman investigations of peptide and protein structure and dynamics. *Chem. Rev. 112*, 2604−2628.
(42) Mikhonin, A. V., Myshakina, N. S., Bykov, S. V., and Asher, S. A. (2005) UV resonance Raman determination of polyproline II, extended 2.51-helix, and β-sheet Ψ angle energy landscape in poly-L-lysine and poly-L-glutamic acid. *J. Am. Chem. Soc. 127*, 7712−7720.
(43) Walsh, S. T. R., Cheng, R. P., Wright, W. W., Alonso, D. O. V., Daggett, V., Vanderkooi, J. M., and DeGrado, W. F. (2003) The hydration of amides in helices; a comprehensive picture from molecular dynamics, IR, and NMR. *Protein Sci. 12*, 520−531.
(44) Mikhonin, A. V., Ahmed, Z., Ianoul, A., and Asher, S. A. (2004) Assignments and conformational dependencies of the amide III peptide backbone UV resonance Raman bands. *J. Phys. Chem. B 108*, 19020−19028.
(45) Shafaat, H. S., Leigh, B. S., Tauber, M. J., and Kim, J. E. (2008) Resonance Raman characterization of a stable tryptophan radical in an azurin mutant. *J. Phys. Chem. B 113*, 382−388.
(46) Wimley, W. C., Hristova, K., Ladokhin, A. S., Silvestro, L., Axelsen, P. H., and White, S. H. (1998) Folding of β-sheet membrane proteins: A hydrophobic hexapeptide model. *J. Mol. Biol. 277*, 1091−1110.
(47) Wong, P. T., Schauerte, J. A., Wisser, K. C., Ding, H., Lee, E. L., Steel, D. G., and Gafni, A. (2009) Amyloid-β membrane binding and permeabilization are distinct processes influenced separately by membrane charge and fluidity. *J. Mol. Biol. 386*, 81−96.
(48) Greenfield, N. J., and Fasman, G. D. (1969) Computed circular dichroism spectra for the evaluation of protein conformation. *Biochemistry 8*, 4108−4116.
(49) Song, S., Asher, S. A., Krimm, S., and Shaw, K. D. (1991) Ultraviolet resonance Raman studies of trans and cis peptides: Photochemical consequences of the twisted π* excited state. *J. Am. Chem. Soc. 113*, 1155−1163.
(50) Brown, M. C., Yakubu, R. A., Taylor, J., Halsey, C. M., Xiong, J., JiJi, R. D., and Cooley, J. W. (2014) Bilayer surface association of the pHLIP peptide promotes extensive backbone desolvation and helically-constrained structures. *Biophys. Chem. 187−188*, 1−6.